Biophysical Chemistry 17 (1983) 35–50
Elsevier Biomedical Press

ELECTRIC DICHROISM OF DNA

INFLUENCE OF THE IONIC ENVIRONMENT ON THE ELECTRIC POLARIZABILITY

Donald C. RAU and Elliot CHARNEY

Laboratory of Chemical Physics, National Institute of Arthritis, Diabetes and Kidney Diseases, National Institutes of Health, Bethesda, MD 20205, U.S.A.

Received 22nd December 1981
Revised manuscript received 26th August 1982
Accepted 26th August 1982

Key words: Electric dichroism; DNA; Electric polarizability; Ion atmosphere polarization; Condensed counterion polarization

In order to test the diffuse ion atmosphere polarization model recently developed by us, the effects of ionic strength, titrating with Mg^{2+} and $Co(NH_3)_6^{3+}$, and coion charge on the electric polarizability of short fragments of DNA are investigated. The results are consistent with the predictions of the theory and show that the diffuse ion atmosphere polarization contributes significantly to the overall orientation of DNA. At low ionic strengths, we attempt to separate the total dipole moment into two components: one that agrees well with the Debye-Hückel ion atmosphere calculations, while the other, presumably due to condensed counterion polarization, appears to be substantially independent of the ionic strength. At higher salt concentrations, however, a simple separation into dipole components is not possible, perhaps due to a significant coupling of ion flows between the diffuse atmosphere and the condensed counterion layer.

1. Introduction

The analysis of structural properties of DNA in solution by electro-optical methods requires an accurate description of the dipole mechanism that generates the orienting torque. Classically, this dipole moment arises from the electric polarization of DNA and its surroundings. Although there is now in the literature a large amount of experimental data concerning the properties of the induced dipole moment of DNA, there is as yet no single theoretical treatment that can adequately embody and correlate these observations. The general consensus is now that the dipole moment is due to the polarization of the surrounding counterions. An exact description of the steady-state distribution of ions surrounding a charged rod is a formidable problem for a polyion as highly charged as DNA.

We have recently calculated the contribution to the dipole moment that would be expected from the polarization of a Debye-Hückel ion atmosphere [1]. Of particular significance with respect to DNA was the finding that this polarizability strongly depends on the charge density of the rod, Q. In particular, if the ionic strength of the solution and the charges of counter- and coions are held constant, then the polarizability along the rod, α_{11}, is proportional to Q^2. Within the framework of Manning's counterion condensation theory [2], it is possible to change significantly the effective charge density of DNA while essentially leaving the ion atmosphere unchanged by titrating a +1 counterion solution with relatively small amounts of +2 or +3 ions. Our approach in assessing the importance of the ion atmosphere polarizability is then two-fold: (1) to compare the magnitude of the observed dipole and its ionic strength and coion dependence with theory; and

(2) to examine the dependence of the observed polarizability on the effective charge density of DNA while holding the ion atmosphere composition essentially constant.

At low ionic strength (≤ 0.5 mM), the observed dipole moment appears to be separable into two independent components, one that is well characterized by the ion atmosphere polarization theory while the other is consistent with Manning's treatment for the polarization of the condensed counterion layer [3]. At higher ionic strengths, however, two simple components are not apparent and the observed orientation is not described adequately by theory. We suggest that in this region interactions between the polarization of the ion atmosphere and the condensed counterion layer lead to the observed behavior.

2. Theory

As stated above, it is generally accepted that the dipole of DNA is a result of the polarization of the surrounding counterions with respect to the charged axially symmetric double helix. The counterion condensation theory of Manning [2] has proved a very useful tool in dealing with DNA-counterion interactions, and provides a good basis to separate counterion polarization into two components. In the theory, counterions are divided into two groups. There is a layer of ions closely associated with or bound to DNA. If the charge of the counterions in solution is Z, then the reduced effective polyion charge density, ξ_{net} (the intrinsic reduced charge density of the polyion minus neutralizing charge density of the bound counterions), is given by,

$$\xi_{net} = \frac{e^2 Q}{DkT} = 1/Z \qquad (1)$$

where Q is the effective linear charge density (in units of numbers of charges/cm), D the bulk dielectric constant, e the electronic charge, k Boltzmann's constant and T the temperature. Surrounding this layer of bound ions is the more conventional diffuse ion atmosphere that can be treated with the familiar Debye-Hückel approximation. Before continuing with a discussion of the various treatments of the polarizations of the condensed layer and diffuse atmosphere, it is first necessary to review the work of Manning on the expected variation of the net charge density in mixed-charge counterion systems.

For an all $Z = +1$ counterion system (e.g., Na^+), eq. 1 predicts that 76% of the DNA phosphate charge is neutralized by bound ions, leaving a net 0.24 charges/phosphate. In an all $Z = 2$ system (Mg^{2+}), however, 88% of the DNA charge should be neutralized, leaving half the net charge density (0.12 charges/phosphate) of the all Na^+ case. In mixed-counterion systems, the effective charge density will vary between these two extremes. Within the framework of his theory, Manning [2] has presented a pair of simultaneous equations that lead to a solution for the effective polyion charge density,

$$1 + \ln\frac{\phi_1}{C_1 V_{p1}} = -2Z_1\xi(1 - Z_1\phi_1 - Z_2\phi_2)\ln\kappa b$$

$$Z_1 + Z_1 \ln\frac{\phi_2}{C_2 V_{p2}} = Z_2 + Z_2 \ln\frac{\phi_1}{C_1 V_{p1}} \qquad (2)$$

where the subscripts 1 and 2 refer to different

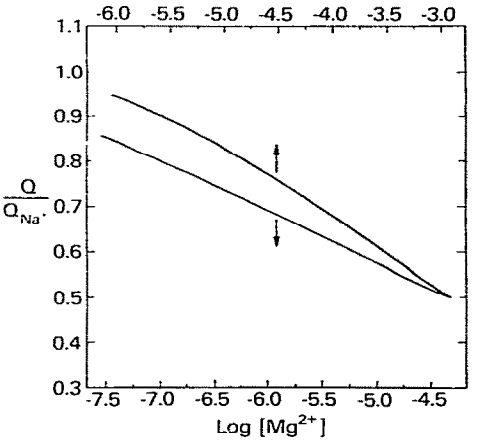

Fig. 1. The theoretically expected variation of the effective DNA charge density, Q, with added Mg^{2+} ($Z = +2$ ions) relative to an all $Z = +1$ charge density is calculated by eq. 2 and shown as a function of $\log[Mg^{2+}]$ for two ionic strengths. In each case, the difference between the Mg^{2+} concentration and the ionic strength is accounted for by added 1 : 1 salt. The upper curve and scale show the calculation for $I = 5$ mM, while the lower curve represents $I = 0.2$ mM.

counterion species and b is the linear DNA phosphate charge spacing, $1/\kappa$ the Debye shielding parameter ($= 3.0/I^{1/2}$, in Å, where I is the ionic strength of the solution), $\xi = e^2/bDkT$, $\phi_{1(2)}$ the number of counterions of species 1 or 2 bound/DNA phosphate, $V_{1(2)}$ the free volume of binding for counterion species 1 or 2, and $C_{1(2)}$ the free (unbound) concentration of species 1 or 2.

Fig. 1 shows the variation of charge density, relative to an all $Z = 1$ system, as a function of $Z = 2$ (Mg^{2+}) concentration for two ionic strengths (each composed of a mixture of Mg^{2+} and Na^+). Two features of these curves are worth noting. First, only very small concentrations of Mg^{2+}, in comparison to the ionic strength, are necessary to change significantly the effective charge density. The composition of the Debye-Hückel ion atmosphere remains essentially all Na^+. Secondly, as the ionic strength is increased it takes proportionately more Mg^{2+} to achieve the same lowered effective charge density.

One aspect of the Na^+-Mg^{2+} equilibrium that is not shown in this figure, but is a consequence of eq. 2, is that at low ionic strengths, most of the DNA charge is neutralized by Mg^{2+}, even at effective charge densities that are only slightly different from the all Na^+ case. We calculate, for example, that for only 78% charge neutralization ($\phi_1 + 2\phi_2$) at $I = 5$ mM ([Na] = 4.992 mM and [Mg^{2+}] = 2 μM, already 32% ($2\phi_2$) is due to condensed Mg^{2+}. How accurately these equations represent the actual change in DNA charge density, however, is not known with certainty. To the best of our knowledge, no systematic study has been done in mixed Na^+-Mg^{2+} systems using a technique that is sensitive to charge density, as, for example, electrophoretic mobility. One troublesome aspect of this equation is that if less than saturating amounts of Mg^{2+} are added (i.e., < 0.38 Mg^{2+}/DNA phosphate), there should be no change in the net charge density. Relaxation time data for T7 DNA [4], however, show a smooth, continuous decrease in the longest relaxation time, at constant ionic strength, up to an added Mg^{2+} concentration of about 0.5 Mg^{2+}/DNA phosphate. The most straightforward explanation for this is that the repulsive electrostatic excluded volume is decreasing, or that the net charge density of DNA is decreasing significantly even at less than saturating amounts of added Mg^{2+}. With this brief background, we can now outline the theoretical work describing the polarization of the ion atmosphere and the condensed layer, with particular emphasis on the expected behavior in mixed counterion systems.

3. Ion atmosphere polarization

The theory developed by us [1] calculates the contribution to the overall dipole amount due to the field-induced distortion of the initial charge symmetry of a Debye-Hückel ion atmosphere and a central, rod-like macroion. In electrophoretic theory, this distortion gives rise to the relaxation field. The particular model we considered was that of a uniformly charged rod of length $2L$ immersed in a medium of dielectric constant D. The supporting electrolyte is a simple Z-Z salt with a number concentration n_0. Solving the standard equations in the Debye-Hückel approximation for the steady-state flow of ions in the externally applied field, the calculated polarizability parallel to the long axis of the rod was found to be,

$$\alpha_{11} = 4D(Z\xi_{net})^2 F(\kappa L)/\kappa^3 \tag{3}$$

The dimensionless function $F(\kappa L)$ is given by,

$$F(\kappa L) = 1/2 \sum_{n=1}^{\infty} \frac{\sin^2(\beta_n \kappa L)}{\beta_n^2 C} \times \left[\frac{(1+2\beta_n^2)}{(1+\beta_n^2)} - 2\ln\left((1+\beta_n^2)/\beta_n^2\right) \right] \tag{4}$$

where it has been assumed that $\kappa a \ll 1$ (where a is the rod radius), $\beta_n = n\pi/C$, and C is large enough such that $F(\kappa L)$ is independent of the Fourier expansion interval $[-C, +C]$. (Eq. 4 is equivalent to eq. 37 of ref. 1 in the limit of $C \to \infty$.) To a good approximation, for $1 \leq \kappa L \leq 6$, the dependence of α on L and κ is given by $\alpha \approx L^{1.85}/\kappa^{1.15}$. There are now a number of studies in the literature reporting an L^2 dependence of the observed dipole moment for short, rod-like fragments of DNA [5–7].

In comparing an all $Z = 1$ (Na^+) counterion environment with an all $Z = 2$ (Mg^{2+}) system, eq.

3 would predict that the ion atmosphere contribution to the dipole moment will not change for a polyion like DNA, given the inverse dependence of ξ_{net} on Z in eq. 1. This result has been observed [8]. In order to investigate the expected behavior in mixed-counterion systems, it is necessary to modify the Z^2 term of eq. 3 to include more than one ion valence. Although lengthy, it is a relatively straightforward matter to show that $\langle Z^2 \rangle$, the average, squared charge of ions in the ion atmosphere (not the condensed counterion layer), is

$$\langle Z^2 \rangle = \frac{\sum_{i=1}^{N} (Z_i^2 n_i)}{\sum_{i=1}^{N} (Z_i n_i)} \qquad (5)$$

where the sum is over all N species of counter- and coions with a charge Z_i and molar concentration n_i in solution. This equation applies only to simple electrolytes; for cases in which there is a dynamic equilibrium between charges (e.g., the phosphate ion at pH 7, a $Z = -1 \leftrightarrow -2$ equilibrium) we have no analogous expression.

Fig. 2 shows an idealized calculation for the

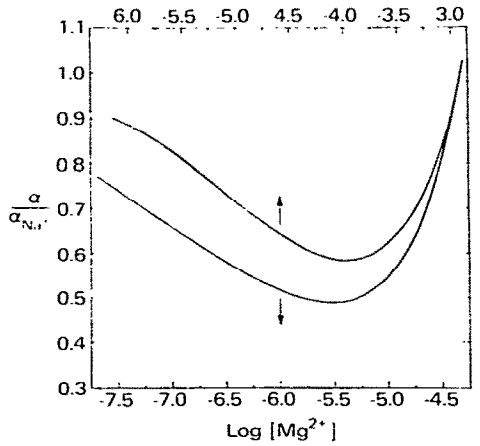

Fig. 2. A theoretical calculation for the expected dependence of the ion atmosphere polarization of DNA relative to an all 1 : 1 salt system on the concentration of added Mg^{2+} (as a 2 : 2 salt) is illustrated for two ionic strengths. As in fig. 1, added 1 : 1 salt maintains the constant ionic strength. The upper curve refers to $I = 5$ mM, while the lower is for $I = 0.2$ mM.

expected dependence of the ion atmosphere dipole moment on Mg^{2+} concentration for two ionic strengths, with a 1 : 1 salt making up the difference. The factor ξ_{net} and $\langle Z^2 \rangle$ in eq. 3 were calculated using eqs. 2 and 5, respectively. There are two trends worth noting in these curves. Most importantly, the polarizability goes through a minimum at very low Mg^{2+} concentrations. This comes about because up to the minimum ξ_{net}^2 is decreasing at a faster rate than the average squared charge of an ion in the ion atmosphere, $\langle Z^2 \rangle$, is increasing. Initially, added Mg^{2+} is preferentially partitioning into the condensed counterion layer, leaving the ion atmosphere essentially all 1 : 1 ions. As the Mg^{2+} concentration is further increased, however, the bound counterion layer becomes saturated with +2 ions, and the excess is displacing 1 : 1 ions in the diffuse atmosphere, at constant ionic strength, until all the ionic strength is from the 2 : 2 salt, which then has the same polarizability as the initial 1 : 1 environment. Secondly, as the ionic strength is increased, the minimum becomes slightly broadly and more shallow and is shifted to slightly higher Mg^{2+} concentrations. This reflects basically the same trend as observed in fig. 1, that at higher ionic strengths, the preferential displacement of +1 ion in the condensed layer by +2 ion is entropically less favorable.

These curves were calculated with the implicit assumption that the DNA phosphate concentration is vanishingly small, certainly much less than the Mg^{2+} concentrations. In real experiments, however, this condition is not often met for the lower range of Mg^{2+} concentrations in fig. 2. In the set of experiments reported here, for example, the DNA phosphate concentration is about 40 μM. This and our previous warning that it is not known for certain how effective charge densities vary with less than saturating amount of Mg^{2+} added prevents a rigorously quantitative comparison of theory and experiment. The trends, however, are important.

3. Condensed counterion polarization

There are several theories in the literature [3,9–12] for calculating the induced dipole mo-

ment of polyion-bound counterions, differing mainly in the treatment of the electrostatic repulsive energy associated with an induced, asymmetric charge distribution. All are equilibrium calculations as opposed to a steady-state flow model. This assumption would be approximately correct if the flow of counterions between the condensed layer and the ion atmosphere, due to the perturbation of that equilibrium, is negligible compared with the flow of counterions along the rod. Although the problem has been recognized [10], most theories also have ignored the influence of the ion atmosphere on the repulsive energies. For this reason, the theory developed by Manning [3] is attractive as a basis for condensed counterion polarization, since the stabilizing influence of the ion atmosphere is included. The treatment is entirely within his condensed counteiron framework and, therefore, compliments the Debye-Hückel ion atmosphere theory. Since the maximal amount of charge shielding by the ion atmosphere is assumed, the final equation represents a maximal equilibrium estimate for the contribution of the bound counterion polarization,

$$\alpha_{11} = \frac{Ze^2\left(1-(Z\xi)^{-1}\right)L^3}{12kTb\left(1-2Z\xi\left(1-(Z\xi)^{-1}\right)\ln\kappa b\right)} \qquad (6)$$

where the various symbols have all been defined elsewhere. At low salt concentrations, the denominator of the term in parentheses is dominated by the $2Z\xi(1-(Z\xi)^{-1})\ln\kappa b$ term, which leads to polarizabilities that: (a) are not dependent on the charge Z of the counterion, which has been observed [8]; and (b) increase slightly with increasing ionic strengths, which is contrary to experimental observations [5–8]. At equilibrium, the polarization of the condensed counterion layer is completely compensated for by the polarization of the ion atmosphere in the opposite direction, since it is implicitly assumed that there is no interaction of the ion atmosphere with the external field, but only with the asymmetric field set up by the polarization of the bound counterions. For this model, then, the system as a whole (DNA, condensed counterions, and ion atmosphere) has no net electrostatic dipole energy. As has been discussed by Fixman [13], in such a case it is more appropriate to consider orienting torques in terms of 'hydrodynamic stress', or differential electrophoresis. In this case, the induced dipole moment will depend on the surface potential gradient, not on the surface charge gradient. For a rod, this will eliminate the slight ionic strength dependence that is in eq. 6.

Although Manning's treatment is for only one charge valence of counterion in solution, it is not difficult to extend qualitatively the analysis to mixed-counterion systems. First, it does not matter that the charges of counter- and coions are in the ion atmosphere, only the overall ionic strength is important. The total energy of interaction of a polarized condensed layer with the field is dependent on the counterion charge and the number bound/DNA phosphate (giving rise to the leading $Z(1-(Z\xi)^{-1})$ factor in eq. 6), whereas the shielding term is dependent only on the effective charge density of DNA. If, as predicted by eq. 2 for the titration of a $Z=+1$ system by $+2$ ions, initially the fraction of bound $+2$ ions is increasing at a faster rate than the net charge density is increasing, then the polarizability would be expected to rise to a maximum, decreasing as the rates of change of ϕ_2 and ξ_{net} reverse.

It is also necessary to discuss qualitatively the interactions between the polarization of the condensed layer and ion atmosphere. Disregarding for the moment the transverse flow of ions between the two, the establishment of any steady-state dipole requires the balancing of ion interactions with the applied electric field, with the relaxation electric field set up by an asymmetric distribution of charges, and the entropic force working against an ion concentration gradient. Since both eqs. 3 and 6 are derived for polarizations that are linear with E, the relaxation fields of each will also be linear with E. The interaction of the ion atmosphere with the relaxation field of the condensed counterions is taken into account in eq. 6, leading to dipole moments that are stabilized by increasing salt concentration. There will also be, however, an interaction between the relaxation field from the ion atmosphere polarization and the unperturbed condensed ion distribution, leading to a back-flow of condensed ions linear with E. Although it is possible to include numerically this effect and calculate

hydrodynamic stresses, it is beyond the scope of this paper which deals with testing the ion atmosphere polarization model. A more serious barrier to simply adding polarization components arises if there is a flow of ions between ion atmosphere and condensed layer that is significant compared with the flow of ions along the rod axis. In such a case, the polarization of neither the condensed layer nor the ion atmosphere can be considered independently but must be treated as a coupled system. It is expected that the transverse flow of ions would increase with increasing bulk ion concentration. We bring this point up since we will show experimentally that the overall dipole does appear to be a simple sum of independent components at low ionic strengths, but if the two components remain at higher ionic strengths then they appear to be coupled.

4. Experimental methods

Two DNA samples are used in the present study. 145 base-pair nucleosomal DNA, isolated from chicken erythrocytes (a gift from Dr. J. McGhee) and sonicated calf thymus DNA, with an average size (as determined by sedimentation velocity) of 240 base-pairs. Both samples were twice phenol extracted at 0.5 M Na^+ and extensively dialyzed against 0.2 M NaCl, 50 mM phosphate buffer (pH ≈ 7.0), 2 mM EDTA, initally, and the final dialyses were with 1 mM phosphate buffer (1.5 mM Na^+, pH 7.0). We found for nucleosomal DNA in particular that without the intial high salt-EDTA dialysis the orientation was much less at low ionic strengths (0.5 mM) than with this step. The nucleosomal DNA was determined to be reasonably monodisperse by gel electrophoresis. Samples for dichroism experiments were prepared by diluting the DNA stocks (in the 1.5 mM Na^+ buffer) into the appropriate salt conditions. All dichroism experiments were performed at 2°C, well below the melting temperature for all the ionic strengths studied. Hexamminecobalt(III), $Co(NH_3)_6^{3+}$, was a gift from Dr. J.A. Schellman. The absorbance at 473 nm was used to determine the concentration of the stock solution [13]. DNA concentrations were calculated using a molar extinction coefficient, at 260 nm, of 6600 M^{-1} cm^{-1}.

4.1. Electric dichroism

The basis apparatus we employ for measuring electric dichroism has been described elsewhere [14]. The two major changes that have been made are: (a) the photomultiplier signal is now processed by a Nicolet 1090AR digital osciloscope interfaced with a Hewlett-Packard 9825A minicomputer for direct data reduction and (b) the square-wave pulse across the Kerr cell is supplied by a Cober (model 606) high power-pulse generator. The polarity of the applied field across is alternated in order to avoid net electrophoresis of the salt and sample. Basically, two different sets of parameters can be obtained in the course of a dichroism experiment. Most important in this study is the linear dichroism, i.e., the change in absorbance, at 260 nm, for light polarized either parallel or perpendicular ($\Delta A_{\parallel}$ and $\Delta A_{\perp}$, respectively) to the applied field, due to the orientation of the DNA. Since our samples are well behaved at all ionic strength, i.e., $\Delta A_{\parallel} = -2\Delta A_{\perp}$, we report only the reduced parallel dichroisms, $-\Delta A_{\parallel}/A$, where A is the isotropic absorbance of the sample at 260 nm. The decay of the dichroism signal after the field is off is also analyzed as part of the experiment. The relaxation kinetics contain important information about the hydrodynamics of DNA. For our purposes, however, decay times are only important in determining whether the changes in electric polarizabilities we observe as the ionic environment is changed are due to changes in DNA dimensions. The results indicate that the changes in decay times are too small to account for the observed dependence of dipole moments on the ionic strength and added Mg^{2+} or $Co(NH_3)_6^{3+}$.

Although Hogan et al. [5] have reported observing abrupt changes in the electric dichroism properties of short DNA fragments at ionic strengths less than about 1 mM, we see no evidence from our own experiments that any significant change in DNA structure occurs in the ionic strength range 0.12–5 mM Na^+, other than changes in the magnitude of the induced dipole moment. We additionally observe no significant dependence of

the orientation on DNA concentration in the range 15–60 μM in nucleotides, nor is there any evidence for any irreversible change in either dichroism or relaxation time induced by the applied field in the course of an experiment.

In the Kerr region, i.e., for field strengths, E, low enough such the reduced parallel dichroism, $\Delta A_{\parallel}/A$, is linearly proportional to E^2, the observed dichroism and the electric polarizability, α, can be related by the standard expression for wholly induced dipole moments [15].

$$-\Delta A_{\parallel}/AE^2 = \alpha/15kT \qquad (7)$$

This makes the reasonable assumption that the polarization along the helix axis is much greater than the polarizations perpendicular to DNA. In calculating theoretical curves for the ion atmosphere polarization, we assume for simplicity that the limiting dichroism of DNA at 260 nm, $(\Delta A_{\parallel}/A)_{E\to\infty}$, is -1.0. It should be mentioned, however, that recent experiments [5,16,17] suggest that this value may be as low as -0.75.

5. Results

Fig. 3 shows a typical experimental set of data for the dependence of the dichroism, $\Delta A_{\parallel}/A$, on the applied field strength, E, for the sonicated calf thymus DNA at 0.25 mM Na^+. As can be easily noted, there is a well defined Kerr region, in which the dichroism is linearly proportional to E^2. In general, the slope of the line in this region can be determined to within 5% error. Within the Kerr region, however, average relaxation times, without more extensive signal averaging, can be determined less precisely, only to about 20% error. For neither the sonicated calf thymus DNA nor the nucleosomal DNA, however, did we observe any qualitative change in the shape of the dichroism vs. E^2 curves at higher field strengths than those shown in fig. 3 that are brought about by the salt environment. For either DNA, the curves for any two ionic strengths can be brought into coincidence by simply scaling the field strengths by the ratio of the observed polarizabilities. This argues against any major change in DNA structure induced by very low ionic strengths, and against any serious degradation produced by sonication.

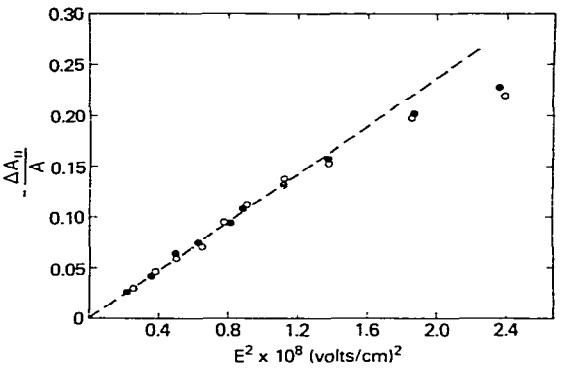

Fig. 3. The results of a typical electric dichroism experiment for the dependence of the parallel reduced dichroism on E^2 are shown. The open and closed circles (○, ●) represent separate experiments on fresh samples of sonicated calf thymus DNA. Each data point is the average dichroism from 4–8 pulses. The experimental conditions are: $[Na^+] = 0.25$ mM ($1/\kappa = 160$ Å), [DNA phosphate] = 30 μM, at 2°C. The best-fitting straight line to the 'Kerr' region is given by the dashed line. The slope of this line ($-\Delta A_{\parallel}/AE^2$) is proportional to the electric polarizability from eq. 7.

5.1. Ionic strength dependence of the dipole moment

In fig. 4, the dependence of the Kerr slopes on the Debye shielding length, $1/\kappa$, is shown for the nucleosomal DNA sample. This approximately linear dependence has been observed by others [4,5]. Still others [6,8], however, have reported a

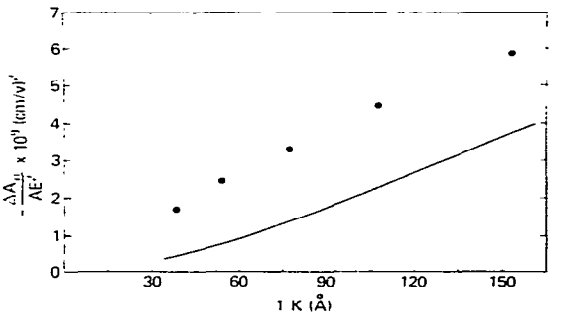

Fig. 4. The dependence of the 'Kerr' slopes (linearly proportional to α) on the Debye shielding length, $1/\kappa$, is shown for the nucleosomal DNA sample. The solid line is the expected contribution from ion atmosphere polarization calculated from eqs. 3, 4 and 7.

somewhat milder dependence of the polarizability on ionic strength, with an approximate $-\ln(\kappa)$ variation. Nonetheless, there is observed a significant inverse dependence of the dipole moment on the ionic strength. In contrast to the results of Hogan et al. [5], as stated previously, we see no sudden and dramatic changes in either the Kerr slope or relaxation times over the entire range of salt concentrations. Further, in contrast to the results of Elias and Eden [6], there is no apparent plateauing of the dipole at very low ionic strengths. In this range of salt concentrations, the average decay time of the dichroism, measured by the area under the decay curve after the end of the pulse, changes by only 20% at the most, with $\langle\tau\rangle = 4.0$ μs. at 2 mM Na^+, indicating that changes in the hydrodynamic length of the DNA are not responsible for the observed variation of the dipole moment with ionic strength.

The solid line in fig. 4 shows the expected Kerr slopes from the polarization of the ion atmosphere alone, calculated from eq. 3 and using a DNA length of 480 Å. As is apparent, this component alone can account for a substantial portion of the overall orientation, from about 24% at 5 mM Na^+ to 64% at 0.27 mM Na^+. Additionally, the slopes of the experimental and theoretical curves are roughly parallel, showing that the theory is correctly predicting the ionic strength dependence. It

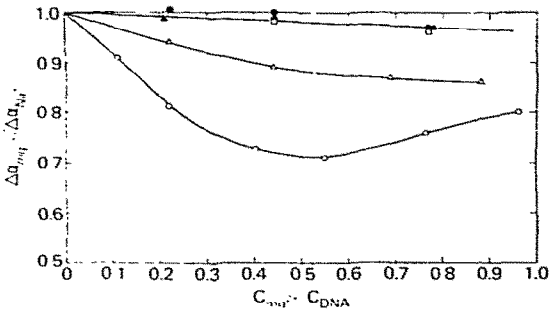

Fig. 5. The ratio of the electric polarizability, observed with added Mg^{2+} to that of the all-Na^+ case is shown as a function of the Mg^{2+} to DNA phosphate concentration ratio. The different symbols correspond to different ionic strengths: (○) $I = 0.37$ mM, (△) $I = 0.74$ mM, (□) $I = 1.48$ mM, (●) $I = 2.95$ mM, (▲) $I = 5.9$ mM.

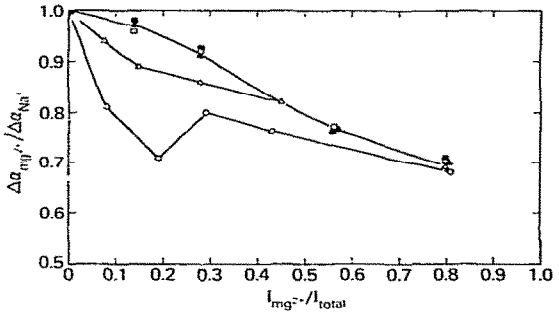

Fig. 6. The ratio of the polarizability with added Mg^{2+} to that observed with an all-Na^+ salt is shown as a function of the relative contribution of Mg^{2+} to the total ionic strength. The symbols, corresponding to different ionic strengths, are the same as in fig. 5.

should be emphasized that once a charge density for DNA is determined by eq. 1, there are no adjustable parameters left in the calculation of the polarizability.

5.2. Mg^{2+} titration

Fig. 5 shows the dependence of the induced dipole moment on the amount of Mg^{2+}/DNA phosphate added, at constant ionic strength. Only at the lowest ionic strength, $I = 0.37$ mM, is there observed a definite minimum, corresponding to an approx. 30% decrease in the polarizability. The four higher salt concentrations show no significant change at all as the condensed layer is titrated with Mg^{2+}, in contrast with all predictions.

A longer range view of the dependence of the dipole on Mg^{2+} concentration, at constant ionic strength, is illustrated in fig. 6, with the relative Kerr slopes plotted as a function of the contribution of Mg^{2+} to the total ionic strength. The three highest ionic strengths follow, within experimental error, the same monotonic decrease in relative polarizability, extrapolating to a limiting value about 40% lower for the all-Mg^{2+} system than for the all-Na^+ case. For $I_{Mg^{2+}}/I_{total} > 0.4$, the relative changes in the dipole moment appear to be coincident for all five ionic strengths. The initial, more rapid decrease in the $I = 0.75$ mM data could possibly represent a shallow minimum superimposed on a decreasing baseline.

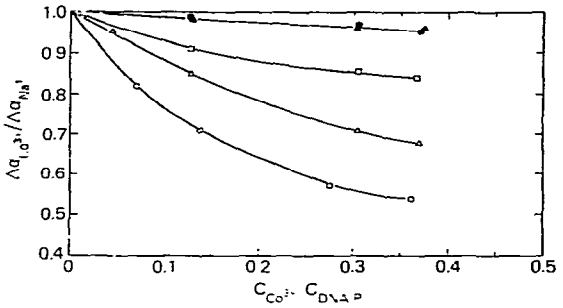

Fig. 7. The change in the electric polarizability of nucleosomal DNA as $Co(NH_3)_6^{3+}$ is added, relative to the all-Na^+ case, is shown as a function of the Co^{3+} to DNA phosphate concentration ratio. The symbols, representing different ionic strengths, are: (○) $I = 0.37$ mM, (△) $I = 0.74$ mM, (□) $I = 1.48$ mM, (●) $I = 2.95$ mM, (▲) $I = 5.9$ mM. For all these ionic strengths, DNA condensation occurs between 0.4 and 0.5 Co^{3+}/DNA phosphate.

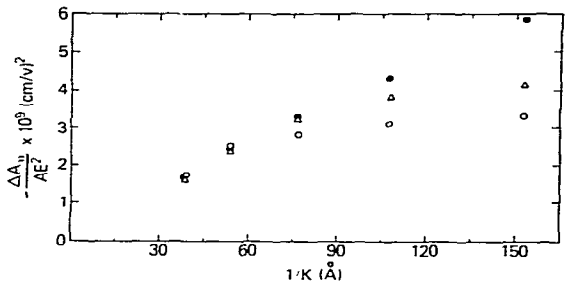

Fig. 8. The dependence of the Kerr slopes on the Debye shielding length, $1/\kappa$, is shown for three cases: (●) all Na^+, (△) approx. 0.5 Mg^{2+}/DNA phosphate added, (○) approx. 0.35 Co^{3+}/DNA phosphate added.

5.3. Co^{3+} titration

The decrease in charge density that accompanies the addition of +2 ions can be further extended with +3 ions, e.g., with $Co(NH_3)_6^{3+}$. As a consequence of further lowering the DNA charge density (cf. eq. 1), however, a barrier is encountered in obtaining a range of Co^{3+} concentrations analogous to that for Mg^{2+} in figs. 5 and 6. Within the Manning condensed counterion framework, it has been shown for +3 spermidine and +3 hexaamminecobalt [13,18] that once approx. 89–90% of the DNA charge has been neutralized, DNA will 'collapse' or precipitate. This critical charge density cannot be obtained with +2 ions in aqueous solution, but is possible with +3 ions. DNA collapse is readily observed with electric dichroism, resulting in large increases in both the polarizability and the relaxation time. The onset of collapse additionally provides an indication that charge densities are changing significantly.

The dependence of the dipole moment, relative to the all-Na^+ case, on the amount of $Co(NH_3)_6^{3+}$/DNA phosphate added, at constant ionic strength, is illustrated in fig. 7. In general, the same trends observed in fig. 5 for the Mg^{2+} titration are also apparent in this case, but are more pronounced. Only at the two highest ionic strengths does the dipole moment remain relatively constant as the proportion of +3 ions is increased. Before DNA collapse (which at these salt concentrations occurs between about 0.4 and 0.5 Co^{3+}/DNA phosphate), the $I = 0.37$ mM polarizability falls approx. 43%; at $I = 0.75$ mM, the decrease is 30%; and finally, at $I = 1.48$ mM, the drop is about 15%. Due to DNA collapse, it is not possible to determine if these curves will reach a minimum, as do the $I = 0.37$ mM data for the Mg^{2+} titration. It is clear, however, that the effect is certainly beginning to saturate at about 0.3 Co^{3+}/DNA phosphate.

A different view of the effect of titrating the condensed layer with +2 or +3 ions is shown in fig. 8. Here the Kerr slopes are plotted as a function of the Debye shielding length for three cases: (a) the all-Na^+ environment, (b) with about 0.5 Mg^{2+}/DNA phosphate added, and (c) with about 0.35 Co^{3+}/DNA phosphate added. Viewed in this manner, it is more apparent that for those ionic strengths that do show a significant dependence of the dipole moment on the charge of the counterion in the condensed layer, the ionic strength dependence of the polarizability is greatly reduced. It is important to note that with the small amounts of Mg^{2+} and Co^{3+} added, the ion atmosphere remains predominately Na^+.

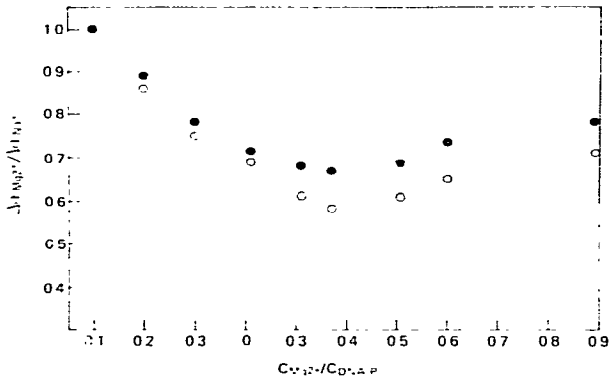

Fig. 9. The ratio of the polarizability with added Mg^{2+} to that of an all-Na^+ system is shown as a function of the Mg^{2+} to DNA phosphate concentration ratio at two ionic strengths, for the sonicated calf thymus DNA sample. The open circles (○) are for $1/\kappa = 230$ Å (0.125 mM Na^+); while the closed circles (●) are for $1/\kappa = 160$ Å (0.25 mM Na^+).

5.4. Mg^{2+} titration at very low ionic strengths

In view of the minimum in the dipole moment observed for the Mg^{2+} titration at $I = 0.37$ mM in fig. 5, it is of interest to examine this region more carefully. To this end, we have looked at the effect of Mg^{2+} titration at very low ionic strengths with

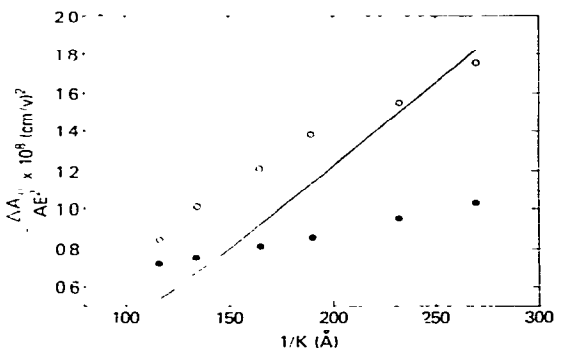

Fig. 10. The dependence of the 'Kerr' slope for the sonicated calf thymus DNA sample on the Debye shielding length, $1/\kappa$, is shown for two cases. The open circles (○) show the results for an all-Na^+ counterion environment; while the closed circles (●) are with 0.5 Mg^{2+}/DNA phosphate added. The solid line shows the expected contribution from the ion atmosphere polarization, calculated with eqs. 3, 4 and 7.

a sonicated calf thymus DNA sample (average length ≈ 800 Å). Fig. 9 shows the dependence of the dipole moment, relative to the all-Na^+ case, on the Mg^{2+}/DNA phosphate ratio, at two ionic strengths. It is readily apparent that the observed polarizability does go through a minimum at about 0.5 Mg^{2+}/DNA phosphate, in qualitative agreement with the $I = 0.37$ mM data in fig. 5. For ionic strengths less than 0.5 mM, the position of the minimum remains constant, but the depth of the well is ionic strength dependent. As was the case with the nucleosomal DNA, as the ionic strength is increased the minimum becomes more shallow.

In a plot analogous to fig. 8, fig. 10 illustrates the dependence of the Kerr slopes on the Debye shielding length for two cases. The open circles give the observed dipole moment with no added Mg^{2+}, the all-Na^+ system; while the solid circles show the change in the Kerr slope when 0.5 Mg^{2+}/DNA phosphate are added, corresponding to the observed minima. In spite of the difference in length between this sample and the nucleosomal DNA and the polydispersity of the sonicated sample, the data in this figure are quantitatively in good agreement with the 145 base-pair sample. At $I = 0.37$ mM, for example, the decrease in the dipole moment from the all-Na^+ case is about 33% when 0.5 Mg^{2+}/DNA phosphate are added for the sonicated sample, while it was about 30% for the nucleosomal DNA. The results of this figure confirm the previous conclusions: that the effect on the polarizability of titrating the condensed layer with $+2$ ions is strongly dependent on the ionic strength, and that for those ionic strengths that are affected by the addition of Mg^{2+}, the apparent dependence of the dipole moment on the Debye shielding length is greatly reduced.

The solid line in fig. 10 represents the expected contribution to the total dipole moment from the ion atmosphere polarization, calculated from eq. 3 for a 1 : 1 salt. Once again, the relative results for this sample are in good quantitative agreement with the nucleosomal DNA. At $I = 0.37$ mM, for example, the ratio of the calculated ion atmosphere dipole moment to the observed is about 0.75 for the calf thymus DNA sample, while it was

about 0.64 from fig. 4. Additionally, except for the two lowest ionic strengths, which appear to be plateauing, the ion atmosphere theory is correctly predicting the slope of the dependence of the dipole moment on the Debye shielding length, to within about 20%. Most importantly, the theoretical calculation shows that ion atmosphere polarization is of the right magnitude to contribute significantly to the observed orientation.

5.5. The effect of coion charge

Eq. 5, derived earlier for the average $\langle Z^2 \rangle$ in a mixed-charge salt solution, underscores the fact that for a Debye-Hückel ion atmosphere a deficit of coions is as important as an excess of counterions in determining the distribution of charge around a central rod. Fig. 11 illustrates the effect of changing the coion charge on the observed dipole moment at three ionic strengths with the calf thymus DNA. In all three cases the coion is also the buffer in solution (pH $\approx$ 7) and is, therefore, not characterized by a fixed valence, but rather is in a dynamic equilibrium between charges. The three coion systems are: (a) cacodylate (a $0 \rightleftharpoons -1$ charge equilibrium), (b) phosphate ($-1 \rightleftharpoons -2$), and (c) citrate ($-2 \rightleftharpoons -3$). Even though a quantitative comparison of theory and experiment is not possible because of the charge equilibrium, qualitatively the results are in accord with the predictions of eqs. 3 and 5. As the charge of the coion is increased, at constant ionic strength, the magnitude of the dipole moment also increases. These data also mesh nicely with the results of the Mg^{2+} titration of fig. 10. The relative effect of the coion charge is significantly greater the lower the ionic strength. At $I = 0.65$ mM, the effect of coion charge is almost negligible (on average about 10%). It is about at this ionic strength that the effect of added Mg^{2+} on the dipole also becomes slight.

An analogous coion dependence has been reported by Charney et al. [8], in comparing the orientation of rod-like fragments in an NaCl solution and in a Mes (2-(*N*-morpholino)ethanesulfonate) buffering system (a $0 \rightleftharpoons -1$ charge equilibrium coion). At very low ionic strengths, the Mes system showed substantially smaller polarizabilities than the NaCl sample, at constant ionic strength, and almost no dependence on the Debye shielding length, whereas with NaCl the ionic strength dependence was about the same as that observed here.

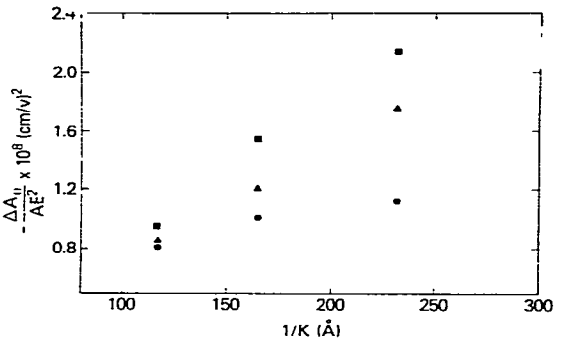

Fig. 11. The influence of coion charge on the 'Kerr' slope at three ionic strengths is illustrated. The symbols, representing different coion buffering systems, are as follows: (■) citrate ($Z = -2, -3$), (▲) phosphate ($Z = -1, -2$), (●) cacodylate ($Z = 0, -1$).

6. Discussion

The decrease in the polarizability in comparing an all-Na^+ system with an all-Mg^{2+} solution in fig. 6 is similar to the results reported by others [5,6,8]. Over the range of ionic strengths examined with nucleosomal DNA (0.37–5.9 mM), the all-Mg^{2+} dipole moments fall to about a fraction 0.60 of the all-Na^+ data, at the same ionic strength. Although the relative changes in comparing Na^+ and Mg^{2+} polarizabilities that have been reported are apparently independent of ionic strength, the magnitude of the fractional decrease at a constant ionic strength does appear to vary with solution conditions. Charney et al. [8], for example, report observing no difference at all in the induced dipole in comparing Na^+ and Mg^{2+} systems. The data of Hogan et al. [5] show an approx. 10–15% decrease in going from Na^+ to Mg^{2+}. Closer to our own observations are the results of Elias and Eden [6], who observe a uniform 50% decrease in the dipole moment in comparing magnesium acetate salt solutions with sodium phosphate buffers, at con-

stant ionic strengths. These differences may represent the coion charge contributions, predicted for the ion atmosphere polarization in eq. 3 and 5 and observed experimentally in fig. 11. On the basis of eq. 1, 3 and 5, no change in the ion atmosphere polarization would be expected in comparing a 1 : 1 salt with a 2 : 2 salt, at constant ionic strength. The theoretically expected ratio of polarizabilities, at constant ionic strength, is 0.75 for comparing a 2 : 1 salt with a 1 : 1 salt, and 0.25 for a 2 : 1 salt relative to a 1 : 2 salt, assuming that the fraction of the DNA charge neutralized by condensation is dependent only on the charge of the counterion. Unfortunately, we cannot quantitatively treat charge effects for buffering coions that are in dynamic charge equilibrium.

In contrast to the monotonic decrease in the dipole moments at high Mg^{2+}/Na^{+} ratios, at low ionic strengths (< 0.5 mM) a well defined minimum is observed at about 0.5 Mg^{2+}/DNA phosphate (figs. 5 and 9). The depth of the well is inversely dependent on the ionic strength of the solution. As a consequence, if the polarizability at about the minimum is plotted as a function of the Debye shielding length (figs. 8 and 10) it appears that the dipole moment is almost independent of salt concentration. As discussed in section 2, a minimum is expected for the polarization of the ion atmosphere when the condensed layer is partially saturated with +2 ions, while the diffuse atmosphere is composed of predominately +1 ions. Initially, +2 ions will preferentially go into the condensed layer, decreasing the effective DNA charge density more rapidly than the average $\langle Z^2 \rangle$ charge in the atmosphere will increase. As the condensed layer becomes saturated with +2 ions, the relative rates of change of the charge density and average $\langle Z^2 \rangle$ will reverse, resulting in a minimum (cf. fig. 2). Large decreases in the observed polarizability as DNA is titrated with small amounts of Mg^{2+} have also been reported by Rau and Bloomfield [4] for very large T7 DNA. The most straightforward way to interpret the data in fig. 10 is to assume that there are two separate components to the dipole moment, ion atmosphere and condensed counterion polarizations, with different ionic strength dependences. If we assume, for example, that the polarization of the condensed layer is independent of the net DNA charge density and the charge of the counterion and that the decrease in the Kerr slope when 0.5 Mg^{2+}/DNA phosphate is added is entirely due to the decrease in the ion atmosphere contribution with an idealized decrease in the effective DNA charge density to $0.5Q_{Na^+}$ (the maximal expected change in going from a +1 to a +2 ion), then fig. 12 can be generated for the contributions of the two components. The open circles represent the dipole moment due to the assumed ion atmosphere polarization (proportional to Q^2) and show a strong ionic strength dependence. The remaining contribution to the total dipole is given by the solid circles. This component appears to be independent of ionic strength in this range of salt concentration, as would be expected on the basis of Manning's treatment for the polarization of the condensed counterion layer. In any treatment of the condensed counterion dipole moment that is coupled with the ion atmosphere, the bulk salt concentration will have two, mutually antagonistic effects to a first approximation. First, with higher

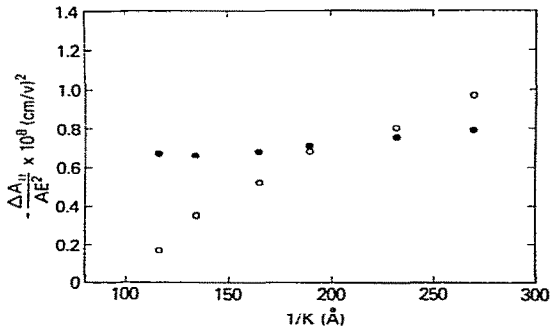

Fig. 12. A separation of the dipole moment for the calf thymus DNA sample at low ionic strengths into two components is shown. It is assumed that the data in fig. 10 can be represented by a simple sum of polarizabilities with $\alpha = \alpha_{CC} + \alpha_{IA}$, for the all-$Na^+$ case, and by $\alpha_{CC} + 1/4\ \alpha_{IA}$ for an added 0.5 Mg^{2+}/DNA phosphate, at the same ionic strengths, where CC stands for condensed counterion and IA for the ion atmosphere. It has also been assumed that the maximal decrease in the effective DNA charge density is observed with 0.5 Mg^{2+}/DNA phosphate i.e., $Q_{Mg^{2+}}/Q_{Na^+} = 0.5$. The open circles (○) show the results for the ion atmosphere contribution, while the closed circles (●) give the remaining, presumably condensed counterion component.

ionic strengths, the net flow of counterions between the condensed layer and the solution will be greater, which decreases the steady-state dipole moment relative to what it would be in the absence of such a flow. Higher ionic strengths, however, will also increase the shielding of the electrostatic energy associated with an induced asymmetric charge distribution. It would not be surprising, therefore, if there was some range of salt concentrations in which these two effects more or less cancelled, leaving the condensed counterion polarization independent of ionic strength.

Alternatively, if we assume that there are once again two components in fig. 10, one that is independent of $1/\kappa$, while the other is described by the ion atmosphere polarization equation, then we can turn the problem around and calculate a ratio of charge densities ($Q_{Mg^{2+}}/Q_{Na^+}$) for the two cases from the relative slopes of the polarizabilities vs. $1/\kappa$. With the observed ratio of 0.30, we calculate that at the minimum $Q_{Mg^{2+}}/Q_{Na^+} = 0.55$, close to the maximal ratio of 0.50.

This view of the simple separation of dipole components is also consistent with the low ionic strength coion results of fig. 11. If the orientation was due entirely to the ion atmosphere polarization, then both the slope of the polarizability vs. $1/\kappa$ and the magnitude of the dipole moment at constant ionic strength would decrease by the same factor, as the charge of the coion is reduced. This is certainly not the case as observed in fig. 11, where, for example, the slope with phosphate as the coion is about a factor of 3.0 times larger than the slope with cacodylate; but the ratios of polarizabilities at constant $1/\kappa$ are significantly less than this value and dependent on the ionic strength. If we assume, however, that there are two components contributing to the orientation, the ion atmosphere polarization and also a condensed counterion dipole moment that is independent of the coion charge, then the results can be explained. Within the framework of the ion atmosphere polarization, a comparison of the relative decreases in the experimentally observed slopes and magnitudes is meaningful only if the coion charge-independent component is subtracted from the data. If, for example, we use the observed factor of 3 difference in the slopes of the dipole moment vs. $1/\kappa$ between the phosphate and cacodylate coion data in fig. 11, then for each ionic strength a 'baseline' component can be determined that brings the ratio of the remaining contribution also to 3. These results are illustrated in fig. 13. Within experimental error, the separation of dipole components is in excellent agreement with the results of fig. 12 for the Mg^{2+} titration data. To arrive at the same result with two such divergent approaches (Mg^{2+} titration and coion charge) is a good indication that the simple separation of the orientation into two independent components, one of which is well described by the ion atmosphere dipole model, is an approximation that can well describe the data at low ionic strengths.

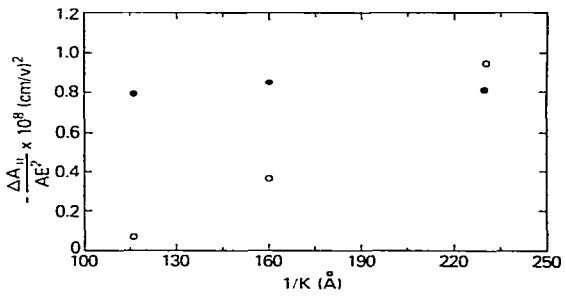

Fig. 13. The data for the dependence of DNA orientation on coion charge in fig. 11 is separated into two components at low ionic strengths, α_{CC} and α_{IA}. It is assumed that α_{CC} is independent of the ionic strengths and of the coion charge, and that α_{IA} is linearly proportional to $1/\kappa$. The ratio of the slopes of $-\Delta A_{\parallel}/AE^2$ vs. $1/\kappa$ in comparing phosphate with cacodylate coions also then gives the ratio of the magnitudes for the ion atmosphere dipole moment, at the same ionic strength, for the two cases. As in fig. 12, the open circles (○) show the contribution from the presumed ion atmosphere dipole, while the closed circles (●) represent the condensed counterion component.

It is not the purpose of this paper to prove one way or another that the second ionic strength-independent component of the dipole moment is to identify strictly with the condensed counterion polarization model of Manning (eq. 6). We have already pointed out that the ionic strength dependence predicted by eq. 6 is in good accord with that observed for the second component. The Kerr slope calculated from eq. 6 for the sonicated DNA sample is approx. 7×10^{-9} (kV/cm)$^{-2}$, in good

agreement with the experimental value of about 8×10^{-9} $(V/cm)^{-2}$ obtained from figs. 12 and 13. Given our qualitative discussion concerning additional factors that we feel should be included in the model, we are not prepared to conclude unequivocally that the salt-independent component of the dipole is correctly given by eq. 6.

Although the data at low ionic strengths can be explained fairly well by the two independent component model, the results are not easily extended to higher ionic strengths or to the $Co(NH_3)_6^{3+}$ titration data. From figs. 12 and 13, the reason why the effect of Mg^{2+} or coion charge is decreasing as the ionic strength is increasing is that the contribution from the ion atmosphere dipole moment, which decreases with increasing salt, is decreasing with respect to the ionic strength-independent component. Extending this reasoning to the nucleosomal DNA data in fig. 4, which overlap quite well with the calf thymus DNA data at low ionic strengths, then it would be expected that for ionic strengths greater than about 0.65 mM the observed dipole moment would be independent of the Debye length. It is certainly clear from fig. 4, however, that this is not the case.

Additionally, the Co^{3+} titration data (fig. 7) provide further evidence that the problem is more complicated that a simple sum of two independent dipole moments would indicate. Given the observation that titrating the condensed layer with Mg^{2+} has negligible effect at ionic strengths greater than about 0.6 mM, due to this calculated small contribution from the ion atmosphere component (figs. 12 and 13), it would be expected that the $Co(NH_3)_6^{3+}$ titration would also show a negligible effect for $I > 0.6$ mM. Fig. 7, however, clearly demonstrates that small amounts of Co^{3+} are effective in decreasing the observed polarizability up to ionic strengths of 1.3 mM. Only at the two highest ionic strengths studied are the observed decreases very small and independent of salt concentration. An analysis of these data in a manner analogous that for fig. 12 would lead to much higher estimates of the ion atmosphere contribution.

The inconsistency of the high ionic strength dependence of the polarizability and the Co^{3+} titration data with the predictions based on the low ionic strength, sum of two independent dipole moments model underscores the discussion in section 2. To consider the ion flows in the diffuse atmosphere and the condensed counterion layer to be totally noninteracting is unrealistic. In our view, the major shortcoming in present theories is that there is no wholly adequate treatment for the condensed counterion dipole moment that incorporates the flow of ions between the condensed layer and the diffuse atmosphere (i.e., a steady-state flow calculation) and the role of the ion atmosphere in shielding the induced asymmetric distribution of condensed counterions. Without such a treatment, for example, since the sum of the charges in the ion atmosphere and condensed layer must be constant (what charge is lost in the ion atmosphere with +2 or +3 ion titration is necessarily gained in the condensed layer), it is not clear whether or not the absence of an observed minimum for the Mg^{2+} titration at $I > 0.6$ mM is due to a cancelling of the expected decrease in the polarization of the ion atmosphere with an increase in the condensed counterion dipole moment. If a steady-state flow theory for the polarization of the condensed layer were available, then the coupling of the dipole moments could be accomplished by simply including linear perturbations terms.

A current view in the literature [19–22] is that the counterion condensation theory of Manning is just a two-state approximation to the real charge distribution that can be adequately described by solving the full (nonlinearized) Poisson-Boltzmann equation. Numerical solutions of the full Poisson-Boltzmann equation for rods as highly charged as DNA do indicate that there is a layer of counterions in a sheath surrounding the rod, the concentration of which is approximately independent of the bulk salt concentration and that the relative net charge density of the rod and sheath varies with the counterion charge in approximately the same manner as predicted by condensation theory (i.e., $Q_{net} \approx 1/Z$). Additionally, the displacement of +1 ions by +2 ions in the sheath for mixed-counterion calculations qualitatively agrees with the results of Manning's theory [22]. With this view, the separation of the small ion charge into diffuse atmosphere and condensed layer seems

very artificial. It would also suggest that a description of dipole moment would be better obtained by solving the complete Poisson-Boltzmann equation with the steady-state flow assumption. This approach will have its own set of problem. Full Poisson-Boltzmann treatments, for example, will tend to underestimate the number of ions close to DNA, since a uniform surface charge density on the rod is generally assumed, whereas DNA phosphate charges are, of course, discrete. As far as we are aware, there is no estimate as to how important an effect this is. It could, however, account for the differences in the concentration of counterions close to DNA as calculated by the full Poisson-Boltzmann treatment and Manning's theory. The problem is also made significantly more difficult than most Poisson-Boltzmann problems because the rod is finite. Finally, to incorporate mixed-counterion charges into the equation will complicate further an already difficult problem. In spite of these potential problems, however, we understand that very promising results have been obtained [23]. We still believe, in any event, that the two-state model of Manning provides a physically simple and appealing basis on which to calculate dipole properties, especially in view of its success in dealing with other problems of DNA electrostatics.

Of primary importance to this work, however, is the demonstration that, at low ionic strengths, experimental observations are consistent with the predictions of the ion atmosphere polarization theory. A comparison of the calculated polarizabilities with observed dipole moments (data in figs. 4 and 10) shows that this component can account for a significant portion of the orientation. It should be emphasized that once the effective charge density of DNA is fixed by counterion condensation theory, then, for a given ionic strength and DNA length, there are no adjustable parameters left in eq. 3. Additionally, the expected decrease in the dipole moment as (a) the condensed layer is titrated with Mg^{2+} or Co^{3+}, while leaving the ion atmosphere predominantly Na^+, and (b) the coion charge is decreased are experimentally observed. These successful tests of the theory support the contention that ion atmosphere polarization is an important component of the overall dipole moment of rod-like fragments of DNA.

The data of Rau and Bloomfield [4] on the electric birefringence of unsheared T7 DNA are even more consistent with the ion atmosphere polarization theory than our own results. Even though eq. 3 was developed specifically for a rod, the induced ion atmosphere dipole of a random coil will show similar behavior with one major difference. In contrast to a rigid rod for which the dipole moment is effectively an end effect (if the charge density is uniform), the charge density of a random coil, in the direction of the field, is Gaussian, and therefore, the field-induced asymmetry of the ion atmosphere will extend throughout the polymer domain. In particular, the dipole force will clearly be global (i.e., the force on any given segment will depend on its distance from the center of mass) and not segmental (the force on a given segment is a function of its orientation in the field, not on its distance from the polymer center). It is not clear if the polarization of the condensed layer would lead to global or segmental orientation forces. The T7 DNA data clearly indicate that the force is global. More importantly, the decrease in the polarizability is very close to the maximal factor of 4 when titrated with Mg^{2+}. Titration with $+3$ ions (spermidine) results in even greater decreases (Rau, unpublished observations) before DNA condensation occurs. For very large (coil-like) DNA, therefore, it seems probable that almost all the dipole is due to ion atmosphere polarization.

7. Concluding remarks

The changes in the observed dipole moment of DNA as a predominately $Z = +1$ counterion solution is titrated with small amounts of $+2$ or $+3$ ions provide a good test in assessing the merits of polarization theories. In particular, it should prove useful in separating the contributions of the diffuse ion atmosphere polarization and the 'condensed counterion' dipole moment, since $+2$ and $+3$ ions are preferentially taken up into the condensed layer. There are four experimental results of this work that are consistent with the predictions of our ion atmosphere polarization theory.

First the calculated magnitudes of dipole moments, with no adjustable parameters once the effective DNA charge density is fixed by Manning's theory, are comparable with the observed values for the two DNA lengths studied. Secondly, the ionic strength dependence is correctly predicted. Thirdly, at very low ionic strengths, the polarizability does go through a minimum as the condensed layer is titrated with Mg^{2+} or Co^{3+}, while the ion atmosphere remains predominately Na^{+}. Finally, also at very low ionic strengths, the theoretically expected dependence of the dipole moment on coion charge was observed.

For ionic strengths less than about 0.5 mM, it appears that the overall polarizability, α, can be represented by a simple sum of independent contributions from the diffuse ion atmosphere, α_{IA}, and the condensed layer, α_{CC}, i.e., $\alpha = \alpha_{IA} + \alpha_{CC}$. At higher salt concentrations, however, either the ion atmosphere polarization becomes negligible or the simplistic assumption that the two components are independent breaks down. In light of the differences between Mg^{2+} and Co^{3+} titrations, it is or opinion that ion atmosphere polarization remains important, but that a complete theory must include the coupling of the two components.

References

1 D.C. Rau and E. Charney, Biophys. Chem. 14 (1982) 129.
2 G.S. Manning, Q. Rev. Biophys. 11 (1978) 179.
3 G.S. Manning, Biophys. Chem. 9 (1978) 65.
4 D.C. Rau and V.A. Bloomfield, Biopolymers 18 (1979) 2783.
5 M. Hogan, N. Dattagupta and D.M. Crothers, Proc. Natl. Acad. Sci. U.S.A. 75 (1978) 195.
6 J.G. Elias and D. Eden, Macromolecules 14 (1981) 410.
7 N.C. Stellwagen, Biopolymers 20 (1981) 399.
8 E. Charney, K. Yamaoka and G.S. Manning, Biophys. Chem. 11 (1980) 167.
9 F. Oosawa, Biopolymers 9 (1970) 677.
10 A. Warashina and A. Minakata, J. Chem. Phys. 58 (1973) 4743.
11 J.M. Schurr, Biopolymers 10 (1971) 1371.
12 J.P. McTague and J.H. Gibbs, J. Chem. Phys. 44 (1966) 4295.
13 M. Fixman, J. Chem. Phys. 72 (1980) 5177.
14 K. Yamaoka and E. Charney, Macromolecules 6 (1973) 66.
15 K. Yamaoka and E. Charney, J. Am. Chem. Soc. 94 (1972) 8963.
16 C.-H. Lee and E. Charney, J. Mol. Biol. (1982) in the press.
17 S. Diekmann, W. Hillen, M. Jung, R.D. Wells and D. Porschke, Biophys. Chem. 15 (1982) 157.
18 R.W. Wilson and V.A. Bloomfield, Biochemistry 18 (1979) 2192.
19 J.A. Schellman and D. Stigter, Biopolymers 16 (1977) 1415.
20 M. Fixman, J. Chem. Phys. 70 (1979) 4995.
21 M. Gueron and G. Weisbuch, Biopolymers 19 (1980) 353.
22 R.W. Wilson, d.C. Rau and V.A. Bloomfield, Biophys. J. 30 (1980) 317.
23 M. Fixman and S. Jagannathan, J. Chem. Phys. 75 (1981) 4048.